International Journal of Thin Film Science and Technology

Volume 4
Issue 3 *Sep. 2015*

Article 2

2015

Annealing Effects on Structural and Optical Properties of Ge10Sb30Se60 Thin Film

M. M. Hafiz
Physics Department, Facility of Science, Assiut University, Egypt., Nahid_abuelhassan2@yahoo.com

N. El-Kabany
Physics Department, Facility of Science, Assiut University, Egypt., Nahid_abuelhassan2@yahoo.com

H. Mahfoz Kotb
Physics Department, Facility of Science, Assiut University, Egypt., Nahid_abuelhassan2@yahoo.com

Y. M. Bakier
Physics Department, Facility of Science, Assiut University, Egypt., Nahid_abuelhassan2@yahoo.com

International Journal of Thin Films Science and Technology

http://dx.doi.org/10.12785/ijtfst/040302

Annealing Effects on Structural and Optical Properties of $Ge_{10}Sb_{30}Se_{60}$ Thin Film

M. M. Hafiz, N. El-Kabany *, *H. Mahfoz Kotb and Y. M. Bakier*.

Physics Department, Facility of Science, Assiut University, Egypt.

Received: 23 Mar. 2015, Revised: 12 May 2015, Accepted: 14 May 2015.
Published online: 1 Sep. 2015.

Abstract: The optical constants of as-prepared and thermally annealed $Ge_{10}Sb_{30}Se_{60}$thin films were determined. Effect of heat treatment on the structure and optical properties of $Ge_{10}Sb_{30}Se_{60}$ thin films in the range between the glass transition and crystallization temperature have been investigated. The glass transition and crystallization temperature of the synthesized sample was measured by non- isothermal DSC measurements. The microstructure and optical properties of these films were characterized by UV-VIS spectrum, scanning electron microscope (SEM) and X-ray diffraction (XRD). The optical band gap for as-prepared and annealed films have been calculated using Tauc's low from the optical transmission and reflection spectra. The results indicate that the optical band gap E_{opt} increases when the annealing temperature (T_a) is lower than the glass transition temperature (T_g), while decreases with further increase of T_a. The XRD studies show that the as-prepared film is amorphous in nature, but the crystalline improved with increasing the annealing temperature. Furthermore the particle size and crystalline increases while the dislocation and strains decreases with increasing the annealing temperature. Thermal annealing was found to be accompanied by structural effects, which in turn, lead to change in the optical constants. The obtained results were explained in terms of the Mott and Davis model for amorphous materials and amorphous to crystalline structure transformations.

Keywords: A. Chalcogenide glasses; C. X-ray diffraction; D. Thermal annealing.

1 Introduction

Thin films of chalcogenide glasses have received a great deal of attention for the last two decades due to their technological applications, namely electronic, optoelectronic, optical and memory switching devices such as optical recording media. As a chalcogenide glass is used as an active component in a particular device, it must be thermally saturated. This is because when such a glass is prepared, generally by melt quenching technique. It is formed in a non-equilibrium thermodynamic state.

Therefore, it is possible that physical properties of a given glass may deteriorate upon usage at temperatures even below the glass transition temperature [1]. Thermal process is known to be important in inducing crystallization in chalcogenide glasses. Chalcogenide semiconductors have truly emerged as multipurpose materials and have been used to fabricate technologically important devices [2-5]. Structural studies of these glasses are important in determining the transport mechanism, thermal stability and practical applications. Annealing of chalcogenide glasses can affect the photo- induced changes, in particular irreversible effects occur in as – deposited films while reversible effects occur in well- annealed films as well as bulk glasses. Changes in local atomic structure are observed on illumination with light having photon energy near the optical band gap of the chalcogenide. Thermal processes are known to be important in inducing crystallization in semiconductor chalcogenide glasses.

The optical storage based on the amorphous- crystalline phase transition utilizes the large optical reflectivity and optical absorption changes obtained in some semiconductors-semimetal thin films by heat treatment [6]. Due to the technological importance , the influence of heat treatment, laser, light- induced changes, ultraviolet irradiation etc, on optical properties and electrical properties of chalcogenide thin films have been subjected to a lot of investigations [7-9]. The decrease of the optical gap E_{opt} by annealing is an interesting behavior especially for optical recording memory system, although it is important in this application to shift the absorption edge sharply. The aim of the present work is to

*Corresponding author E-mail: Nahid_abuelhassan2@yahoo.com

investigate the possibility of using thin films of Ge10Sb30Se60 thin film as phase change recording media which could be viewed through the optical and structural properties.

Optical absorption measurements and structure investigation have been carried out on as – deposited and thermally annealed film. Scanning electron microscope (SEM) and X-ray diffraction were used to determine the structural changes for the studied composition.

2 Experimental Technique

Chalcogenide glasse of $Ge_{10}Sb_{30}Se_{60}$was prepared by the melt- quenched technique. The high – purity elements were weighted according to their atomic percentages and were sealed in evacuated silica tubes, which were heated at 1200^0C for 15h. The ampoules were frequently rocked at maximum temperature to insure the homogeneity of the melt. The quenching was performed in ice water. Thin films were prepared by thermal evaporation under vacuum of 10^{-5}Torr using an Edwards E-306 coating system. The evaporation rates as well as the film thickness were controlled by using a quartz crystal monitor FTM 5.

In order to determine the absorption coefficient α and the optical constants of the films as a function of the incident light wavelength, the transmittance T(λ) and reflectance R(λ) were recorded at room temperature using a double- beam spectrophotometer (Shimadzu UV-210 combined with PC)

The glassy nature of the as- prepared as well as the crystalline phase structures for annealed samples was identified using an X-ray diffractometer (Philips, PW 1710), with Cu as a target (λ=1.54178A^o), at 40kV and 30 mA with scanning speed 2^o min^{-1}. DSC experiments were carried out on the as- prepared powder sample under non- isothermal conditions. The surface morphology of the films was examined using scanning electron microscopy (SEM) Technique Jeol (JSM)-T200 type. The values of the glass transition temperature T_g , the onset crystallization temperature T_c and the peak crystallization temperature T_p were determined with accuracy ±1K using the microprocessor of the thermal analyzer

3 Results and discussion

3.1 Structural analysis

The glassy as well as amorphous nature of $Ge_{10}Sb_{30}Se_{60}$ composition was verified by non- isothermal Differential Scanning Calorimetric (DSC) measurements at a constant heating rate of 10K/min (shown in Fig.1). The DSC thermo grams are characterized by two temperatures; the glass transition temperature (T_g) as defined by the endothermic change in the DSC trace which represents the strength or rigidity of the glass structure. Indicates a large change of viscosity, marking a transformation from amorphous solid phases to super cooled liquid state. The other exothermic peak temperature known as crystallization temperature (T_c) originating from the amorphous- crystalline transformation is used to identify the crystallization process.

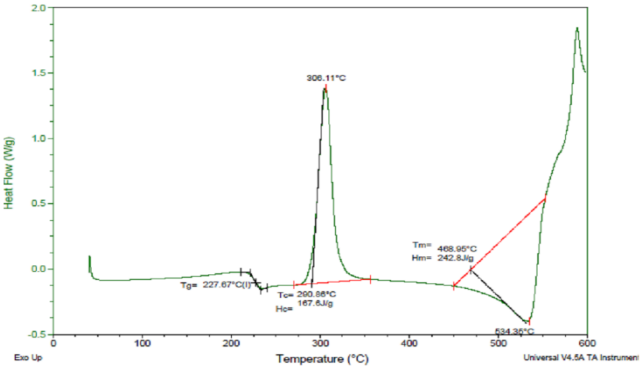

Figure 1: DSC trace for the powdered $Ge_{10}Sb_{30}Se_{60}$ chalcogenide glass at 10K/min.

It is observed from Fig.1, the studied composition have single endothermic and exothermic peaks, indicates this material is in glassy nature as well as in amorphous nature and are homogeneous. The glass transition temperature T_g and the crystallization temperature T_c equals to 550K and 563K respectively. The annealing temperature has been selected from these DSC thermo grams and is in between glass transition temperature (T_g) and crystallization temperature (T_c) of the prepared sample.

The X-ray diffraction technique was employed for studying the structural details of $Ge_{10}Sb_{30}Se_{60}$ thin film deposited on glass substrate.

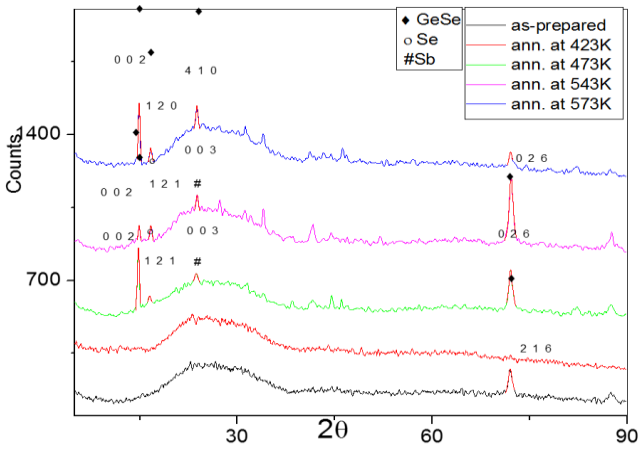

Figure 2: X-ray pattern of $Ge_{10}Sb_{30}Se_{60}$ chalcognide thin films: as-deposited and annealed at different temperature.

Fig.2 shows the X-ray diffraction traces of as- prepared and annealed thin film. The absence of sharp structural peaks for as- prepared film confirms the (amorphous nature). While the XRD pattern of the $Ge_{10}Sb_{30}Se_{60}$ thin film at different annealing temperature (423K, 473K, 543K and 573K) shows the formation of some crystalline phases confirms (partially crystalline structure), the crystalline increases with increasing the annealing temperature. These results are in

good agreements with the previously reported results [10, 11] .It is expected for amorphous materials that the increase of crystalline is associated with a decrease in energy gap.

The individual crystallite grain size in the film has been determined using the Scherer's formula as [12]

$$\text{Grain size } (D) = S\lambda/\beta\cos\theta \quad (1)$$

Where λ is the wavelength of the X-ray (1.5406Å), β is the width of a strong peak at half – maximum intensity (FWHM) and θ is the corresponding Bragg diffraction angle and the Scherer constant (S) is of the order of unity.

Using the crystallite grain size, the dislocation density δ, defined as the length of dislocation line per unit volume of the crystal and the strain values of as-prepared and annealed $Ge_{10}Sb_{30}Se_{60}$ have been evaluated.

The strain values (ε) were calculated using the equation [13]

$$\varepsilon = \left(\frac{\lambda}{D\cos\theta} - \beta\right)\left(\frac{1}{\tan\theta}\right) \quad (2)$$

The dislocation density (δ) has been calculated using the following formula [14]:

$$\delta = \frac{n}{D^2} \quad (3)$$

Where n is a factor, which equals unity giving minimum dislocation density. The number of crystallites per unit surface area N can be determined through the following relation [15]

$$N = \frac{t}{D^3} \quad (4)$$

Where t the thickness of the films

The grain size D, strain (ε) and dislocation density (δ) for all annealed films have been calculated using above formula and the values are given in Table 1.

The comparison of the observed atomic spacing, d and the slandered values for as deposited and annealed films is given also in Table 1. It is observed that the average particle size increases with increasing the annealing temperature ≥ 543 K after that it decreases with annealing temperature ≥ 573. But the dislocation density and the strain have the opposite trend. This result indicates that, thermal annealing of amorphous solids at temperatures higher than the glass transition temperature causes crystallization. The amount of the thermally transformed crystalline phase increases with increasing annealing temperature. It is suggested that when the dislocation density is fairly high there is an increase in band gap of the semiconductor material because of the presence of dislocation provided that the dislocations are separated by a distance greater than the inter-atomic distance [15].

The SEM investigation of the present work shows the presence of crystalline phases after annealing at temperatures ≥ 473K, as shown in Fig3.

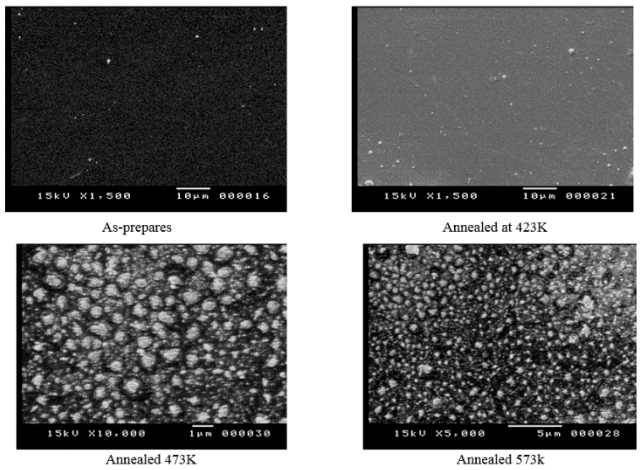

Figure 3: (a-d) SEM micrographs of $Ge_{10}Sb_{30}Se_{60}$thin films: as-prepared and annealed at 423,473 and 573K.

The scanning electron microscope image of the deposited film shows micro-crystallites for the investigated sample. We have observed a clear change in the morphology of the films during thermal annealing.

3.2 Optical analysis

The most interesting optical processes in thin films are the absorption and emission light, absorption permits a determination of the optical band gap of the semiconductor and it generates charge carriers [16]. It is possible to separate three distinct regions in the absorption edge spectrum of amorphous semiconductors. The first is the weak absorption tail, which originates from defects and impurities. Second is the exponential edge region, which is strongly related to the structural randomness of the amorphous compound. Third is the high absorption region from which optical energy gap width can be determined .

The band tails width of localized states (E_t) near the band edges can be calculated using Urbach's empirical relation [17]

$$\alpha(\upsilon) = \alpha_o \exp(h\upsilon / E_t) \quad (5)$$

Where α_o is a constant, and E_t is the Urbach energy, hυ is the photon energy and α (υ) is the absorption coefficient. From the Urbach energy, the steepness parameter σ which characterizes the broadening of the absorption edge due to the electron-phonon interaction or excitation- phonon interaction can be calculated using the relation.

$$\sigma = k_B T / E_t \quad (6)$$

Where k_B is Boltzman constant and T is the absolute temperature.

The optical energy gap, E_{opt} and the type of optical transition

Table 1: Structural parameters for the thermally evaporated $Ge_{10}Sb_{30}Se_{60}$ for deposited and annealed thin films

$Ge_{10}Sb_{30}Se_{60}$	d_{stand}	$d_{exp.}$	h	k	l	Kind of Phase	Particle size D (nm)	Average of particle size for GeSe phase(nm)	Strain	Average of stain values for GeSe phase	Dislocation density $\delta x10^{15}(m^{-2})$	Average of dislocation density $\delta x10^{16}$ for GeSe phase
as-prepeared	1.31	1.31	2	1	6	GeSe	11.78	11.782	0.0013	0.00134	7.20	0.0072
Annealing.at 473K	5.95	5.95	0	0	2	GeSe	14.24	13.487	0.0050	0.00314	4.93	0.00555
	5.35	5.32	1	2	1	Se	12.69		0.0050		6.21	
	3.74	3.74	0	0	3	Sb	11.57		0.0038		7.46	
	1.31	1.31	0	2	6	GeSe	12.73		0.0012		6.17	
Annealing at 543K	5.92	5.93	0	0	2	GeSe	18.74	16.207	0.0038	0.00311	2.85	0.00382
	5.35	5.30	1	2	1	Se	14.91		0.0042		4.50	
	3.74	3.74	0	0	3	Sb	15.29		0.0029		4.27	
	1.31	1.31	0	2	6	GeSe	13.68		0.0011		5.30	
Annealing at 573K	6.03	6	0	0	2	GeSe	14.05	15.164	0.0050	0.00318	5.06	0.00466
	5.38	5.37	1	2	0	GeSe	16.98		0.0037		3.47	
	3.76	3.75	4	1	0	GeSe	17.59		0.0025		3.23	
	1.31	1.31	0	2	6	GeSe	12.03		0.0013		6.91	

responsible for optical absorption, (direct or indirect) have been determined by Tauc relations. It is states that [18]

$$(\alpha h\upsilon) = ß\,(h\upsilon - E_{opt})^r \quad (7)$$

Where β is a constant, hυ the photon energy, E_{opt} the optical energy gap, α the absorption coefficient, and r a constant which depends on the type of the electronic transitions.

The reflectivity of an absorbing medium of indices n and k under normal incidence is given by [19, 20]

$$n = \frac{1+R}{1-R} + [(\frac{1+R}{1-R})^2 - (k^2 - 1)]^{1/2} \quad (8)$$

Where k is the absorption index and λ, the incident light wavelength.

$$k = \frac{\alpha\lambda}{4\pi}$$

The dielectric constant represents the ability of material to polarization is given by the relation

$$\varepsilon = \varepsilon_1 - i\varepsilon_2 \quad (9)$$

The real and imaginary part of dielectric constants ε_1 and ε_2 are related to n and k values through the relation [21]:

$$\varepsilon_1 = n^2 - k^2 = \varepsilon_\infty - (\frac{e^2 N}{4\pi^2 c^2 \varepsilon_0 m^*})\lambda^2 \quad (10)$$

And

$$\varepsilon_2 = 2nk = (\frac{\varepsilon_\infty \omega_p^2}{8\pi^2 c^3 \tau})\lambda^3 \quad (11)$$

Where ε_∞ is the high frequency dielectric constant, ω_p is the plasma frequency, τ the dielectric relaxation time. The real part of the dielectric constant relates to dispersion, whereas dissipative rate of the electromagnetic wave in the dielectric medium is provided by imaginary part.

3.2.1 Optical properties during phase transformation

The effect of thermal annealing on the optical properties of $Ge_{10}Sb_{30}Se_{60}$ thin film has been studied. The thermal annealing process was performed under vacuum for half an hour at temperature (423K, 473K, 543K and 573K). The optical band gap of the film under investigation has been calculated from the knowledge of the reflection and transmitting data obtained from the spectro-photometric measurements. This part includes the results of transmission and reflectance measurements and their relation to wavelength. From these measurements it can be calculated many optical constants, like (absorption coefficient, refractive index, extinction coefficient, dielectric constant, volume and surface energy loss functions).

3.2.2 Transmission and Reflectance measurements

The transmission (T) and the reflection (R) spectra of the as- deposited and thermally annealed $Ge_{10}Sb_{30}Se_{60}$ thin film as a function of annealing temperature and wavelength in the range (200- 2500nm) are shown in Fig. (4.a, b).

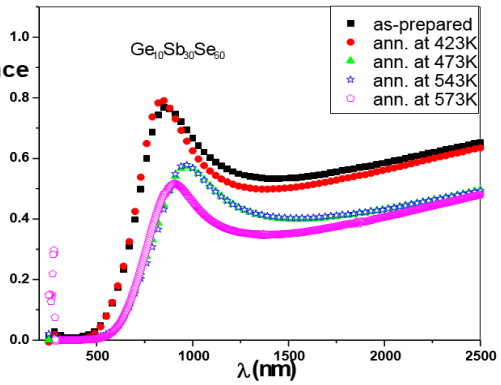

Figure 4(a): The spectral transmittance (T) for as – prepared and annealed $Ge_{10}Sb_{30}Se_{60}$ film.

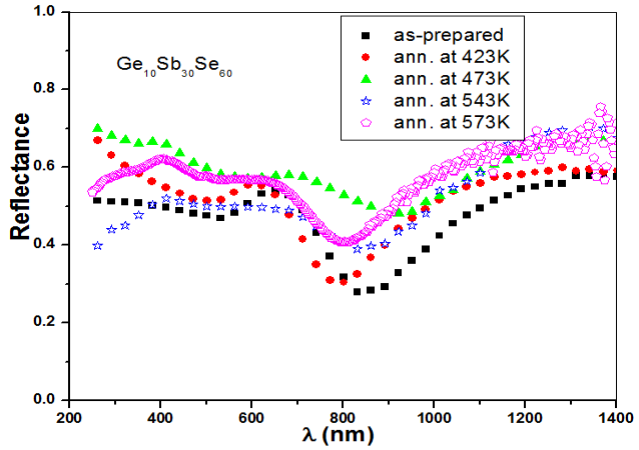

Figure 4(b): The spectral reflectance (R) for as – deposited and annealed $Ge_{10}Sb_{30}Se_{60}$ film.

It is observed that the transmission increase with increasing the wavelength and the peak relative transmitting have maximum value around (800nm) and shift to higher wavelength for the film annealed at 543K. It is also noticed that the film transparency decreases but the film reflectance increases with increasing the annealing temperature.

3.2.3 Absorption coefficient measurements

The effect of heat treatment on the tail width of localized state E_t and optical gap E_{opt} of the of $Ge_{10}Sb_{30}Se_{60}$ thin film have been studied by heating the as prepared film at different temperature for half an hour. Urbach energy E_t has been calculated from the reciprocal slope of the linear portion of a plot of ln (α) versus photon energy. Fig. (5.a) shows this relation for as- deposited and annealed films at different annealing temperatures.

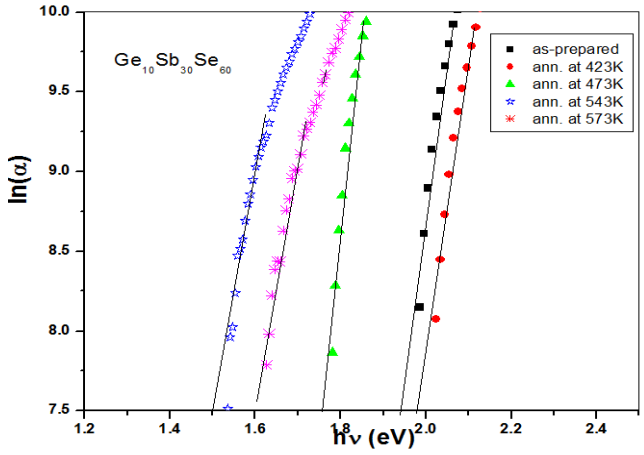

Figure 5(a): The relation between ln(α) vs hυ for as – prepared and annealed $Ge_{10}Sb_{30}Se_{60}$ film.

Also the steepness parameter σ has been calculated from Eq(6), this parameter characterizes the broadening of the absorption edge due to the electron-phonon interaction or excitation- phonon interaction.

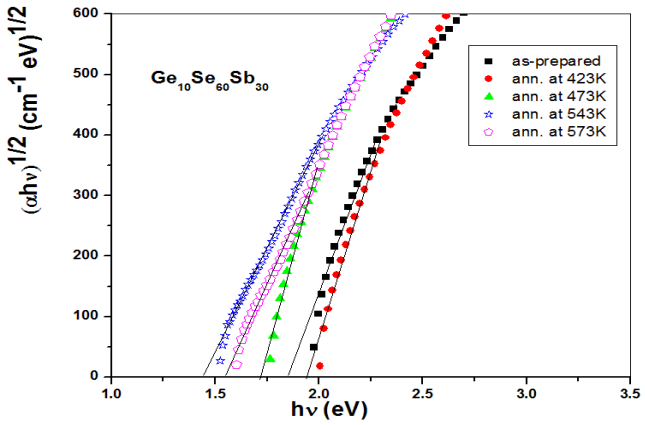

Figure 5(b): The relation between $(\alpha h\upsilon)^{1/2}$ vs hυ for as – prepared and annealed $Ge_{10}Sb_{30}Se_{60}$ film.

According to Tauc's relation for indirect transition, Fig (5.b) shows a plot of $(\alpha h\upsilon)^{1/2}$ versus photon energy, hυ for as-deposited and annealed films at different annealing temperatures.

The values of the optical band gap E_{opt}, the Urbach energy E_t and the steepness parameter σ for the as prepared and annealed films are given in Table 2.

The dependence of E_{opt} on the annealing temperature of the $Ge_{10}Sb_{30}Se_{60}$ films is shown in Fig.6.

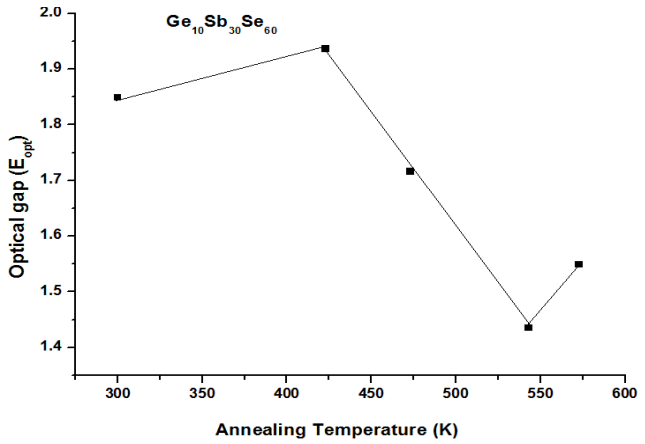

Figure 5: The dependence of optical gab with the annealing temperature for $Ge_{10}Sb_{30}Se_{60}$ film.

It is noticed that E_{opt} increases slightly as annealing temperature T_a increases up to 400K i.e. ($T_a \leq T_g$) the annealing temperature lower than the glass transition temperature T_g, and a decrease in the E_{opt} followed annealing at the temperature 473 and 543 K ($T_a \geq T_g$). Finally, a slow increase was observed due to annealing at temperatures 573K. The steepness parameter has the same trend indicates that the absorption edge changes with annealing. But the Urbach energy has the opposite trend of the optical gap.

The initial increase in the optical band gap due to annealing the as- deposited film of $Ge_{10}Sb_{30}Se_{60}$ at temperature $T_a \leq T_g$ can be explained in terms of the density of states model

proposed by Mott and Davis for amorphous materials [22]. Half an hour of annealing at T≥ 400K results in minor arrangements of the constituent atoms which reduces the defects existed in the as- prepared films and causes the slight increase in the optical gap.

Table 2: Optical properties for as-prepared and annealed $Ge_{10}Sb_{30}Se_{60}$thin films

Temperature	E_{opt} (eV)	E_t (eV)	σ	ε_∞	N/mx10^{51} ($m^{-3}Kg^{-1}$)
As-prepared	1.8488	0. 406	0.0629	59.736	6.59509
423K	1.9355	0. 335	0.076396	56.816	6.4182
473K	1.7155	0. 500	0.051148	106.339	10.7878
543K	1.4355	1.011	0.025284	161.526	22.2344
573K	1.54888	0. 92	0.0278	167.359	24.045

The observed decrease of the optical gap for $Ge_{10}Sb_{30}Se_{60}$ films with the annealing temperatures higher than the glass transition temperature (Ta>Tg) can be explained as a result of amorphous - crystalline transformation. The major change in the optical energy gap after thermal annealing could be attributed to the thermally induced crystalline phase [23].

The reduction in the optical gap can be explained according to Hesegawa et al suggestion [24, 25]. They suggested that the unsaturated bonds are responsible for the formation of localized tail states in the band gap. The presence of a high concentration of these states is responsible for the decrease of E_{opt} in the as- deposited films. This transformation is accompanied by an increase in grain size; therefore, the drastic effect of crystalline phases on optical gap can by explained as a result of the production of surface dangling bonds around the crystallites during the crystallization process [26]. Further increase of annealing temperature results in the breaking up of the formed crystallites into smaller crystallites, thereby increasing the number of surface dangling bonds responsible for the formation of some types of defects. These defects lead to the decrease of the optical gap.

Our results indicates that the optical gap decreases and the grain size increases , the dislocation density and the strain decreases with increasing the annealing temperature as a result of amorphous to crystalline transformation, this agreement with the above discussion .

3.2.4 Refractive index (n) and extinction coefficient (k)

The refractive index n and the extinction coefficient k of the sample can be obtained from eq. (8). The spectral dependence of the refractive index, n and extinction coefficient, k on the wavelength λ for as deposited and annealed $Ge_{10}Sb_{30}Se_{60}$ thin films are shown in Fig (7a, b).

It is observed that the value (n_{max}) at wavelength λ_c decreases with increasing wavelength beyond the absorption edge and shifted to higher wave length with increasing the annealing temperature. This may be due to the change in crystallite size, and the decreasing of optical band gap with increasing the annealing temperature [27].

The extinction coefficient, k defines several different measures of the absorption of light in a medium. By definition, the extinction coefficient is the imaginary part of the complex index of refraction which also relates to light absorption. It is observed that the extinction coefficient increases with increasing the annealing temperatures. This type of trend has been also observed for thin films of various other semiconductors [28, 29]. The increase of ,n and k with increasing annealing is caused by an increase in the particle size with annealing temperature ,which can be explained as, chalcogenide thin films always contain a high concentration of unsaturated bonds or defects [30].

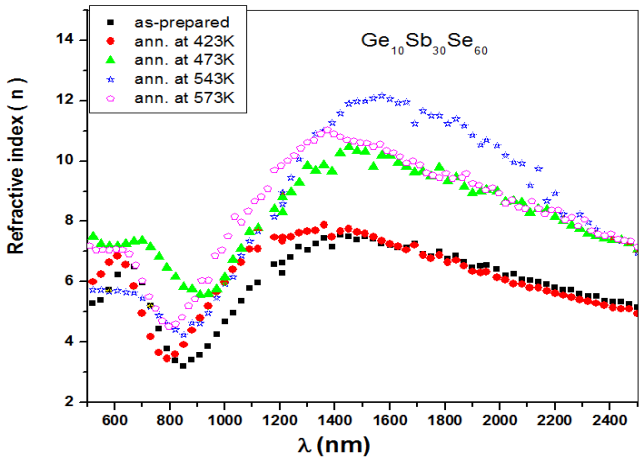

Figure 6(a): the relation between refractive index(n) and wavelength (λ) for $Ge_{10}Sb_{30}Se_{60}$ film.

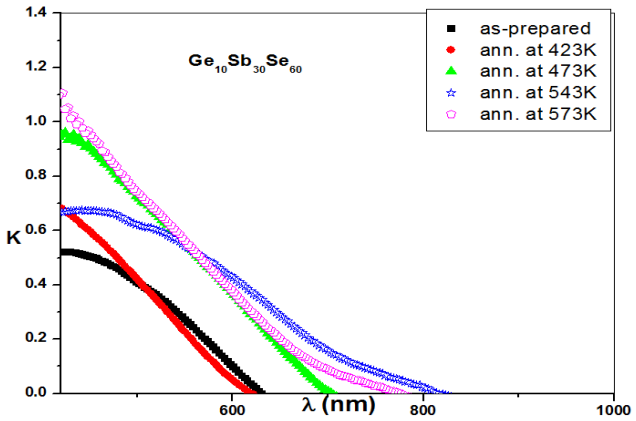

Figure 7(b): the relation between the extinction coefficient (k) and wavelength (λ) for $Ge_{10}Sb_{30}Se_{60}$ film.

During thermal annealing at temperature below the crystallization temperature, the unsaturated defects are gradually annealed out producing a large number of saturated bonds. The reduction in the number of unsaturated defects decreases the density of localized states in the band structure consequently increasing the extinction coefficient.

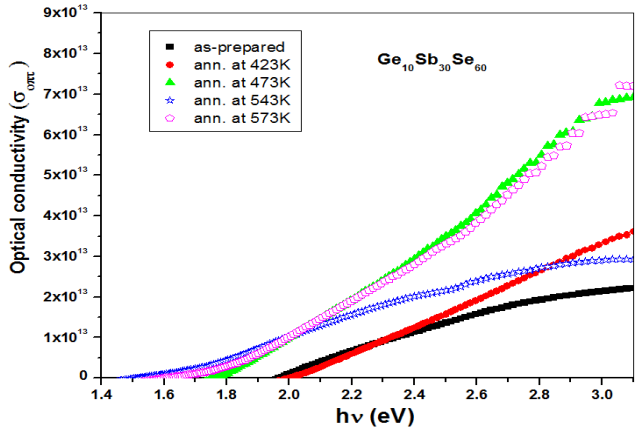

Figure 7: the relation between the optical conductivity (σ_{opt}) and the photon energy (hυ) for $Ge_{10}Sb_{30}Se_{60}$ film.

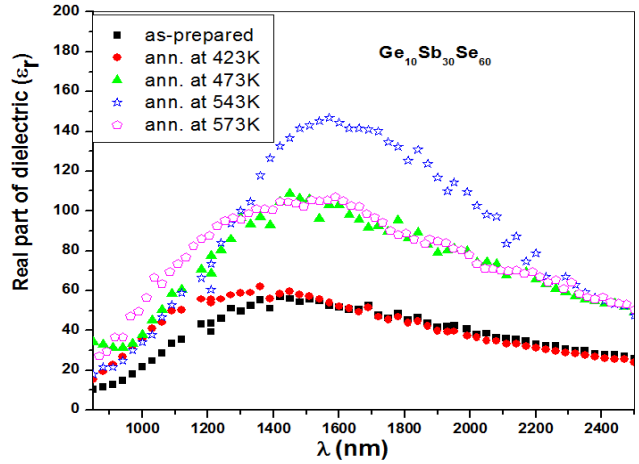

Figure 8(a): The relation between Real part of dielectric constant (ε_r) and the wavelength for $Ge_{10}Sb_{30}Se_{60}$ film.

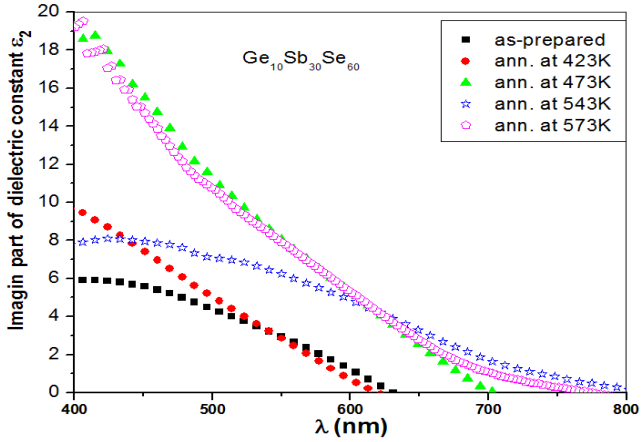

Figure 9(b): The relation between imagin part of dielectric constant (ε_r) and the wavelength for $Ge_{10}Sb_{30}Se_{60}$ film.

3.2.5 Optical conductivity

Among the different quantities that are used to characterize the optical properties of thin films is the optical conductivity, σ_{opt}, that are commonly calculated as follows [31]

$$\sigma_{opt} = \frac{\alpha nc}{4\pi} \qquad (12)$$

Where α is the absorption coefficient and c is the velocity of light.

The variation of the optical conductivity as a function of photon energy for as prepared and annealed films is shown in Fig (8). It is noticed that the optical conductivity increases with increasing the photon energy and annealing temperature. This may be a result of the high absorbance of thin films and/or is due to the excess electrons emitted by means of photon energy. The value of optical conductivity for the as prepared film is in the range of ($2x10^{18}$) and for the annealed film at 573K is in the range of ($7x10^{18}$) at room temperature , this attributed to annealing caused by the high rearrangement of ions and inside the lattice and includes crystalline evaluation.

3.2.6 Dielectric constant

For a better understanding of the optical properties of the as-prepared and annealed films, it is necessary to determine some optical constants such as real and imaginary parts of dielectric constant .The dependence of real part ε_1 and imaginary part ε_2 of dielectric constant with wavelength for as prepared and annealed films for $Ge_{10}Sb_{30}Se_{60}$ shown in Fig (9 a,b) . The real part of the dielectric constant (ε_1) associated with the term that how much it will slow down the speed of light in the material .The imaginary part gives that how a dielectric absorb energy from electric field. The values of real and imaginary parts of the dielectric constant depend on refractive index (n) and extinction coefficient (k).

Furthermore, in order to calculate the lattice dielectric constant ε_∞, we have further analyzed the data of refractive index dependence on the wavelength. The dependence of n^2 on λ^2 is linear at longer wavelength as shown in Fig.10. Extrapolating the linear part of this dependence to zero wavelengths gives the value of ε_∞ and from the slopes of these lines we can calculate the values of N/m* for as prepared and annealed films where N is the free carrier concentration and m* the effective mass of the charge carriers. The values of ε_∞ and N/m* are given in Table.2. It is noticed that the values of these two parameters increases with increasing the annealing temperature. This behavior was observed in many chalcogenide glasses. In general, it can be concluded that high frequency dielectric constant ε_∞ and the ratio N/m* are related to the internal microstructure.

3.2.7 Volume and surface energy loss functions

Energy absorption by the material which might be due to single electron transitions or to collective effects induced within the solid can be expressed in terms of the volume (-Im (1/ε)) and surface (-Im (1/ (ε_{+1}))) energy loss functions which describe the probability that fast electrons will lose energy when traveling the bulk and surface of the material,

respectively.

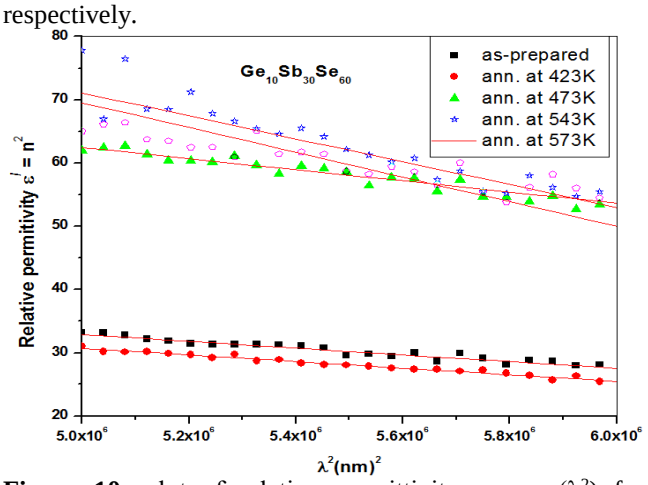

Figure 10: plot of relative permittivity versus (λ^2) for $Ge_{10}Sb_{30}Se_{60}$ film.

The energy- loss functions are related to real and imaginary part $\varepsilon_1$and ε_2 of the complex dielectric constant by the following relations [32]:

$$-I_m\left[\frac{1}{\varepsilon}\right]=\left[\frac{\varepsilon_1}{(\varepsilon_2^2+\varepsilon_1^2}\right] \quad (13)$$

$$-I_m\left[\frac{1}{\varepsilon+1)}\right]=\left[\frac{\varepsilon_1}{(\varepsilon_2+1)^2+\varepsilon_1^2}\right] \quad (14)$$

Fig. (11 a, b) illustrates the dependence of both volume and, surface energy loss functions on the photon energy (hυ).

It is clear that the two functions in general increase with increasing the photon energy and annealing temperature. In additions, the energy loss by the free charge carriers when traversing the bulk material has approximately the same value as when traveling the surface in particular for relatively lower energies but the energy lost by the bulk volume of such films is greater than that lost by the surface at higher energies.

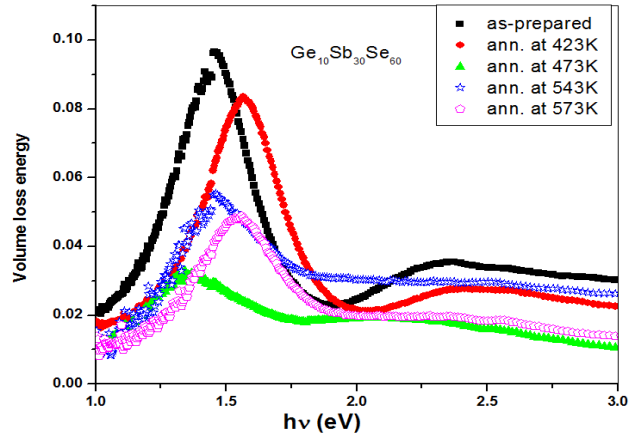

Figure 11(a): volume energy loss vs photon energy hυ for $Ge_{10}Sb_{30}Se_{60}$ film.

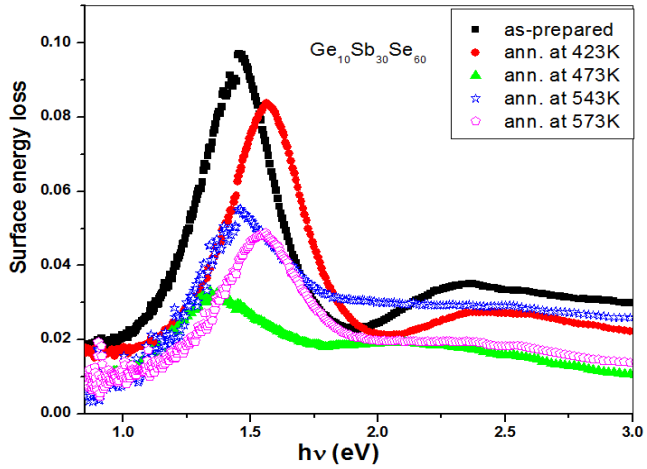

Figure 11(b): Surface energy loss function vs photon energy hυ for $Ge_{10}Sb_{30}Se_{60}$ film.

4 Conclusion

From the above results and discussion the following conclusion can be made:

-The annealing temperature affects the structure and optical properties of $Ge_{10}Sb_{30}Se_{60}$ thin film.

-The X-ray analysis showed that the as-deposited film has an amorphous nature.

-Annealing the as-deposited $Ge_{10}Sb_{30}Se_{60}$ films at different temperature showed amorphous to crystalline transition.

- The average particle increased whereas the dislocation and strains decreased with increasing the annealing temperature.

-The allowed non- direct transition successfully describes the absorption mechanism in the as-prepared and annealed films.

-The optical gap increased with increasing annealing temperature Ta up to the glass transition temperature T_g and hence remarkable decrease in the values of E_{opt} occurred with further increasing of annealing temperature Ta>Tg.

-This behavior was explained in terms of the Mott and Davis model for amorphous materials and amorphous to crystalline structure transformations.

-An Understanding of amorphous to crystallization phase transformation in these chalcogenide thin film is very important to develop them for advanced applications based on the amorphous to crystallization phase change.

References

[1] MMA.Imran, IF.Al-Hamarneh, Mi.Awadallah, MA.Al-Ewaisi, *Physica.B.* **403**, 2639, (2008).

[2] H.Nasu, J.D.Mackenzie, *Opt Eng* **26**,102, (1987).

[3] W.Leung, N.W.Cheung, A.R.Neureuther, *Appl. Phys. Lett.* **46**, 481, (1985).

[4]J. Feinleib, J. DeNeufville, S. C.Moss, S. R.Ovshinsky, *Appl.Phys.Lett.* **18**, 254, (1971).

[5] J. PDeNeufville, S.C. Moss, S.R. Ovshinisky, J. *Non-Cryst. Solids.* **13,** 191, (1973).

[6] A. Lafi Omar, MA. Imran Mousa, *Radiat. Phys Chem.* **79,** 104, (2010).

[7] A. Bahishti Adam, MA.Majeed Khan, BS.Patel, FS.Al-Hazmi, M.Zulfequar, *J. Non-Cryst Solids*, **355**, 314, (2009).

[8]Rk. Pan, HZ. Zang, TJ. Zhang, XJ. Zhao, *Physica B* **404,** 3397, (2009).

[9] E. Marquez, R. Jimenez-Garay, JM. Gonzalez-Leal. *Mater Chem. Phys.* **115,** 751, (2009).

[10] Zhang Yunxia, Li Guanghai, Zhang Bo, Zhang Lide, *Materials Letters*. **58**, 2279, (2004).

[11] Gu Yifeng, Song Zhitang, Zhang Ting, Liu Bo, Fang Songlin, *Solid- State Electronics* **54,** 443, (2010).

[12]S. Subramanian, D. P. Padiyan, *Mate. Chem. Phys.* **107**, 392, (2008).

[13] D. Pathinerttam, A. Padiyan, K. R. Murali, *Mater.Chem.Phys.***78,** 51, (2002).

[14] N.Tohge, T.Minami, M.Tanaka. *J. Non-Cryst. Solid* **59**, 999, (1983).

[15]R.Sathyamoorthy, J. Dheepa, *J. Phys. Chem. Solids* **68,** 111, (2007).

[16] J.Pankove, J. I, "Optical process in semi conducting thin films", *Thin Solid Films*, Vol. **90**, pp.172, (1982).

[17] F. Urbach, *Phys. Rev*, **92,** 132, (1953).

[18] J. Tauk, R. Grigorovici, A. Vancu, *Phy. Sta. Solidi.* **15,** 627, (1966).

[19] D. P. Gosain, T. Shimizu, M. Suzuki, T. Bando, S. Okano, J. *Mater Sci.* **26**, 3271, (1991).

[20] N. Sharoff, A.K. Chakravati, *Opt. Memories Technol- orgies and Apple.* **7**, 83, (1991).

[21] D.J.Gravesteijn, *Appl. Opt.* **27**, 736, (1988).

[22] N. F. Mott, E. A. Davis, Electronic Process in Non-Crystalline Materials Clarendon, Oxford, (1979).

[23] S.Hasegawa, S.Yazaia, T.Shimizu, *Solid State Commun*. **26,** 407, (1978).

[24] S.Hasegawa, S.Yazaki, *Solid State Commun.* **23,** 41, (1977).

[25] S.Hasegawa, M.Kitagawa, *Solis State commun.* 27, 855, (1978).

[26]S. Choudhari, S. K. Biswas, *J. Non-Cryst Solids*, **54,** 179, (1983).

[27] P. Sharma, V. Sharma and S. C. Katyal, *Chalcogenide letters*, Vol. **3**, No.10, 73, (2006).

[28] H. Mahfoz Kotb, M. A. Dabban, A. Y. Abdel-Latif, M. M. Hafiz, *J. Alloys Comp.* **512**, 115, (2012).

[29] F. S. Al-Hazmi, *Physica* **B404**, 1354, (2009).

[30] E.Bertan, A.Lousa, *Sol. Energy Mater* **17,** 55, (1988).

[31]Y. Caglar, S. Ilican and M. Caglar, *Eur Phys*, J.B, **58,** 251, (2007).

[32] I. Jacques, Pankove, Optical process in semiconductors, New York: Dover publication institute, (1971).